Article

Smad1/5/8 are myogenic regulators of murine and human mesoangioblasts

Domiziana Costamagna[1,2], Mattia Quattrocelli[1], Florence van Tienen[3], Lieve Umans[4,5], Irineus F. M. de Coo[6], An Zwijsen[4], Danny Huylebroeck[5,7], and Maurilio Sampaolesi[1,8,*]

[1] Translational Cardiomyology Laboratory, Stem Cell Biology and Embryology, Department of Development and Regeneration, KU Leuven, Leuven, Belgium
[2] Laboratory of Experimental Medicine and Clinical Pathology, Department of Clinical and Biological Sciences, University of Turin, Turin, Italy
[3] Department of Clinical Genetics, Maastricht University Medical Center, Maastricht, The Netherlands
[4] Laboratory for Developmental Signalling, VIB Center for the Biology of Disease, Department of Human Genetics, KU Leuven, Leuven, Belgium
[5] Laboratory of Molecular Biology (Celgen), Department of Development and Regeneration, KU Leuven, Leuven, Belgium
[6] Department of Neurology, Erasmus MC-Sophia Children's Hospital, Rotterdam, The Netherlands
[7] Department of Cell Biology, Erasmus MC, Rotterdam, The Netherlands
[8] Division of Human Anatomy, Department of Public Health, Experimental and Forensic Medicine, University of Pavia, Pavia, Italy
* Correspondence to: Maurilio Sampaolesi, E-mail: maurilio.sampaolesi@med.kuleuven.be

Mesoangioblasts (MABs) are vessel-associated stem cells that express pericyte marker genes and participate in skeletal muscle regeneration. Molecular circuits that regulate the myogenic commitment of MABs are still poorly characterized. The critical role of bone morphogenetic protein (BMP) signalling during proliferation and differentiation of adult myogenic precursors, such as satellite cells, has recently been established. We evaluated whether BMP signalling impacts on the myogenic potential of embryonic and adult MABs both *in vitro* and *in vivo*. Addition of BMP inhibited MAB myogenic differentiation, whereas interference with the interactions between BMPs and receptor complexes induced differentiation. Similarly, siRNA-mediated knockdown of *Smad8* in *Smad1/5*-null MABs or inhibition of SMAD1/5/8 phosphorylation with Dorsomorphin (DM) also improved myogenic differentiation, demonstrating a novel role of SMAD8. Moreover, using a transgenic mouse model of *Smad8* deletion, we demonstrated that the absence of SMAD8 protein improved MAB myogenic differentiation. Furthermore, once injected into α-Sarcoglycan (Sgca)-null muscles, DM-treated MABs were more efficacious to restore α-sarcoglycan (αSG) protein levels and re-establish functional muscle properties. Similarly, in acute muscle damage, DM-treated MABs displayed a better myogenic potential compared with BMP-treated and untreated cells. Finally, SMADs also control the myogenic commitment of human MABs (hMABs). BMP signalling antagonists are therefore novel candidates to improve the therapeutic effects of hMABs.

Keywords: BMP signalling, mesoangioblast, pericytes, skeletal muscle, regeneration, SMAD

Introduction

Murine and human mesoangioblasts (MABs) are pericyte-derived cells and represent an intriguing source of multipotent stem cells located in the adult muscle tissue around small vessels (Dellavalle et al., 2007), or in the embryo around the dorsal aorta (Tonlorenzi et al., 2007). These pericytes can be prospectively isolated from freshly dissociated alkaline phosphatase

(AP$^+$) cells of both mouse and human samples (Quattrocelli et al., 2012) and proliferate *in vitro* under specific culture conditions. When transplanted into animal models for muscular dystrophies (MDs), MABs have been demonstrated to colonize host muscles and revert the dystrophic phenotype (Sampaolesi et al., 2003, 2006; Dellavalle et al., 2007; Chun et al., 2013). Indeed, these muscle progenitors, which intrinsically differ from satellite cells (SCs), display trans-endothelial migration when systemically injected (Tedesco and Cossu, 2012) and are currently tested in a phase-1 clinical study in Duchenne Muscular Dystrophy (DMD) patients (EudraCT #2011-000176-33).

The mechanisms inducing MABs to differentiate towards skeletal muscles are still poorly defined. Recently, we showed that Delta-like ligand 1 (Dll1)-activated NOTCH1 and downstream MEF2C support MAB myogenic commitment *in vitro* and *in vivo* (Quattrocelli et al., 2014). However, other signalling pathways

involved in pathological processes in MDs, such as fibrosis, inflammation, and regeneration, still need to be elucidated. Nuclear factor-κB (NF-κB) and transforming growth factor-β1 (TGFβ1) pathways have already been connected to dystrophic muscle degeneration in DMD patients and mouse models (Bernasconi et al., 1995; Chen et al., 2005; Acharyya et al., 2007; Christov et al., 2007; Cohn et al., 2007).

Here, we investigate whether bone morphogenetic protein (BMP)–SMAD signalling could play a role in regulating MAB myogenic capacity. BMPs are secreted factors able to activate specific BMP receptor complexes (BMPRs) that phosphorylate intracellular SMAD effector proteins (i.e. SMAD1, SMAD5, SMAD8), as well as non-SMAD signalling-dependent protein kinases (Feng and Derynck, 2005). After translocation to the nucleus, activated SMADs bind to DNA and regulate specific target genes, including the *Inhibitor of differentiation/DNA binding* (*ID*) genes (Katagiri et al., 2002). Indeed, IDs sequester and inactivate ubiquitous E-box binding proteins thereby hampering their binding with tissue-specific E-family transcription factors such as MyoD and myogenin, which are necessary for the entire muscle differentiation programme (Jen et al., 1992). Previous studies have demonstrated that the receptor-mediated phosphorylation of SMAD1/5/8 (P-SMAD1/5/8) guides the stemness of SCs and modulates their differentiation (Ono et al., 2011). Furthermore, the inhibition of BMP signalling in adult healthy muscles is responsible for muscle atrophy, influencing a specific ubiquitin ligase (Sartori et al., 2013).

Here, using different approaches, we demonstrate how the inhibition of SMAD-mediated BMP pathway promotes the contribution of MABs to the formation of myotubes. Surprisingly, genetic inhibition of *Smad1/5* did not affect the myotube formation *in vitro*. However, additional silencing of *Smad8* resulted in enhanced myogenic differentiation. The injection in dystrophic mice of MABs with reduced SMAD signalling improved the functional recovery of the dystrophic phenotype. We also found that MABs from both embryo and adult mice, as well as from human, act similarly. Notably, we provide evidence that the myogenic commitment of human MABs (hMABs) is under the control of SMAD1/5/8; perturbation of this control has an impact on human MAB myogenic differentiation ability.

Results
Murine MAB growth and differentiation

Adult MABs (aMABs) carrying GFP were co-cultured with C2C12 cells and induced to differentiate by serum starvation. After 5 days of differentiation, double-positive GFP$^+$/ MyHC$^+$ myotubes were detected by immunofluorescence (IF) analysis (Figure 1A and B). The growth curves of GFP$^+$ primary murine MABs and C2C12 murine myogenic cells are shown in Figure 1C and H. The differentiation was confirmed by WB analysis (Figure 1D), where MyHC was again detected on Day 5 of differentiation. The absence of MyHC in aMAB cultures confirmed that adult murine MABs do not spontaneously undergo myogenic differentiation (Quattrocelli et al., 2014). The quantification of the amount of MyHC reported an increment in co-culture conditions with respect to C2C12 cells (Figure 1E). Interestingly, this improvement in differentiation was also observed in co-culture

experiments with embryonic MABs (eMABs, Figure 1F–J) and dystrophic MABs (dMABs), an aberrant model of cardiac mesoangioblasts isolated from *β-Sarcoglycan*-null mice (dMABs; Crippa et al., 2011) (Supplementary Figure S1). Altogether, these data confirm that murine MABs improve the myogenic differentiation of C2C12 cells.

BMP signalling regulates MAB differentiation

BMP signalling is relevant to SCs maintenance (Ono et al., 2011) and its importance for eMABs has been suggested in a previous report, wherein Noggin, a secreted inhibitor of BMP ligands, was shown to promote myotube differentiation (Ugarte et al., 2012). IF analyses of GFP$^+$ aMABs co-cultured with C2C12 cells showed nuclear expression of both P-SMAD1/5/8 and ID proteins in GFP$^+$ aMABs on Day 0 (Figure 2A). On Day 3 of differentiation (Figure 2B), a reduction of P-SMAD1/5/8 and ID nuclear staining was observed, mainly in GFP$^+$ multinucleated cells, suggesting that a decreased BMP signalling is necessary to promote myotube formation. These results were verified by WB analysis (Figure 2C and Supplementary Figure S2A, B). Similar data were confirmed in co-cultures of eMABs, where the levels of P-SMAD1/5/8 and ID proteins were almost completely decreased in eMABs when cells were co-cultured in differentiation medium for 3 days (Figure 2D–F).

Taken together, these results support that BMPs and downstream BMP–SMAD signalling maintain the stemness of both embryonic and adult MABs, and that inhibition of this pathway is required to trigger myotube formation.

Gain and loss-of-function studies

We reported that aMABs are not able to form spontaneously myotubes and the permanent treatment with Noggin, an acknowledged BMP antagonist (Reshef et al., 1998; Linker et al., 2003; Tzahor et al., 2003), or Dorsomorphin (DM), a synthetic inhibitor of type I BMP receptor complex (Hao et al., 2008; Yu et al., 2008) cannot sort any myogenic effects (Figure 3A and B). However, BMP4 was able to induce MAB proliferation as documented by the increased number of Ki67-positive cells (Figure 3B and E). To understand the impact of BMP signalling on the differentiation of MABs into myotubes, we transiently (48 h) treated co-cultures of C2C12 cells and aMABs with BMP4 (Figure 3C and F) or eMABs (Figure 3D and G) (Katagiri et al., 1997; Dahlqvist et al., 2003). In parallel, we transiently treated co-cultures with Noggin or DM. After 5 days of myogenic differentiation, no GFP$^+$/MyHC$^+$ myotubes were present in any of the co-cultures exposed to BMP4 (Figure 3C and D). In contrast, co-cultures treated with Noggin or DM showed high presence of double-positive myotubes, indicating that blockade of BMP signalling has a strong differentiation-inducing effect (Figure 3C and D). Finally, the calculated fusion index in the chimeric myotubes confirmed that no differentiation was detected when the co-cultures were pre-treated with BMP4, whereas a significant increment was noticed in co-cultures treated with Noggin or DM (Figure 3F, G and Supplementary Figure S2C–E). The co-culture experiments in which MABs alone were exposed to BMP4, Noggin, or DM (Supplementary Figure S3A–C), and in which differentiation was induced by adding C2C12 cells after treatment, focused on addressing the critical role of BMP signalling in MAB myogenic commitment.
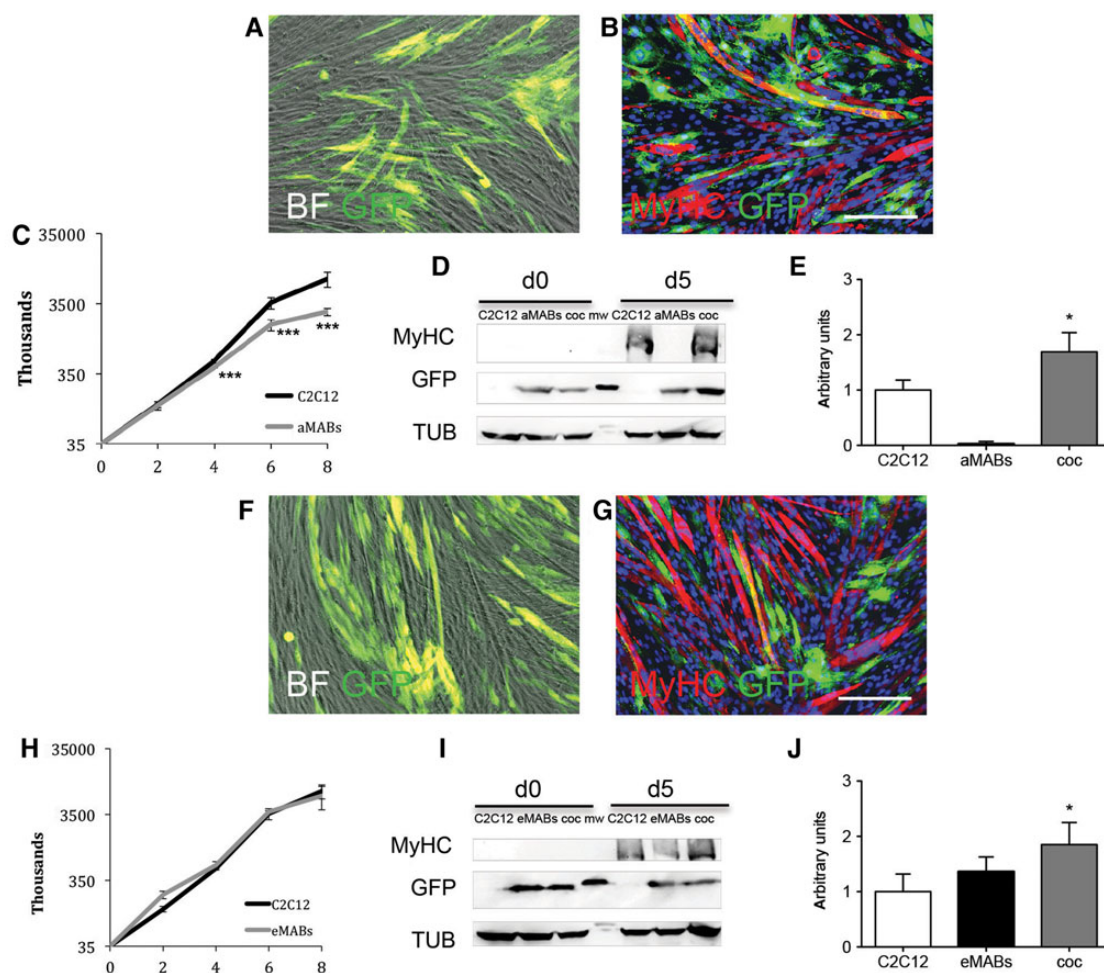
Figure 1 Myogenic differentiation of adult mesoangioblasts (aMABs) and embryonic mesoangioblasts (eMABs). (**A**) Merged images (phase-contrast and GFP signal) of GFP[+] aMABs co-cultured with C2C12 cells (1:1 at the start) in differentiation medium on Day 5. (**B**) IF for MyHC and GFP (respectively in red and green). Nuclei were stained in blue with Hoechst. (**C**) Growth curves of aMAB (grey line) and C2C12 (black line) cell cultures under growing conditions, respectively. (**D**) WB for MyHC, GFP, and tubulin (TUB) in C2C12, aMABs, and co-cultures (coc) of aMABs and C2C12 (1:1) on Day 0 and 5 of differentiation. (**E**) Quantification for the levels of MyHC normalized by TUB in C2C12, aMABs, and co-cultures on Day 5 of differentiation. (**F**) Merged images (phase-contrast and GFP signal) of GFP[+] eMABs co-cultured with C2C12 (1:1) in differentiation medium on Day 5. (**G**) IF analysis for MyHC and GFP (respectively in red and green). Nuclei were stained in blue with Hoechst. (**H**) Growth curves of eMAB and C2C12 cultures under growing conditions, respectively. (**I**) WB for MyHC, GFP, tubulin (TUB) in C2C12, eMABs, and co-cultures of eMABS and C2C12 (1:1) on Day 0 and 5 of differentiation. (**J**) Quantification for the levels of MyHC normalized by TUB in C2C12, eMABs, and co-cultures on Day 5 of differentiation. Data are representative of three independent experiments and values are expressed as mean $\pm$ SD; *$P < 0.05$, ***$P < 0.001$ vs. C2C12. Scale bar, 500 μm.

Moreover, DM administration under differentiating conditions also resulted in increased myotube formation (Supplementary Figure S4A–D). These results highlight the importance of BMP signalling in maintaining MAB stemness (Supplementary Figure S5A–C) and the necessity of inhibition of this BMP effect (Supplementary Figure S5D and E) in order to proceed further along the myogenic route.

Smad1/5 depletion is not sufficient to improve myogenic differentiation

Mouse embryos deficient in type I receptor *ALK-1* (activin receptor-like kinase-1, known to bind primarily BMP, and also TGFβ, on endothelial cells) exhibit delayed differentiation of vascular smooth muscle cells with their consequent failure to localize to peri-vascular regions (Oh et al., 2000). Moreover, *Smad5*-knockout embryos have enlarged blood vessels with decreased numbers of vascular smooth muscle cells, and these embryos die around E10.5–11.5 due to defects in the circulatory system (Chang et al., 1999; Yang et al., 1999; Goumans and Mummery, 2000). The difference in severity of the phenotypes between ligand, receptor, and *Smad*-deficient mice suggests that, in the case of BMPs in particular, other receptors and ligands may partially compensate for the loss of one protein (Pangas et al., 2008; Beets et al., 2013). In order to define the role of different BMP-SMADs in pericytes, we investigate the differentiation ability of MABs isolated from adult mice and
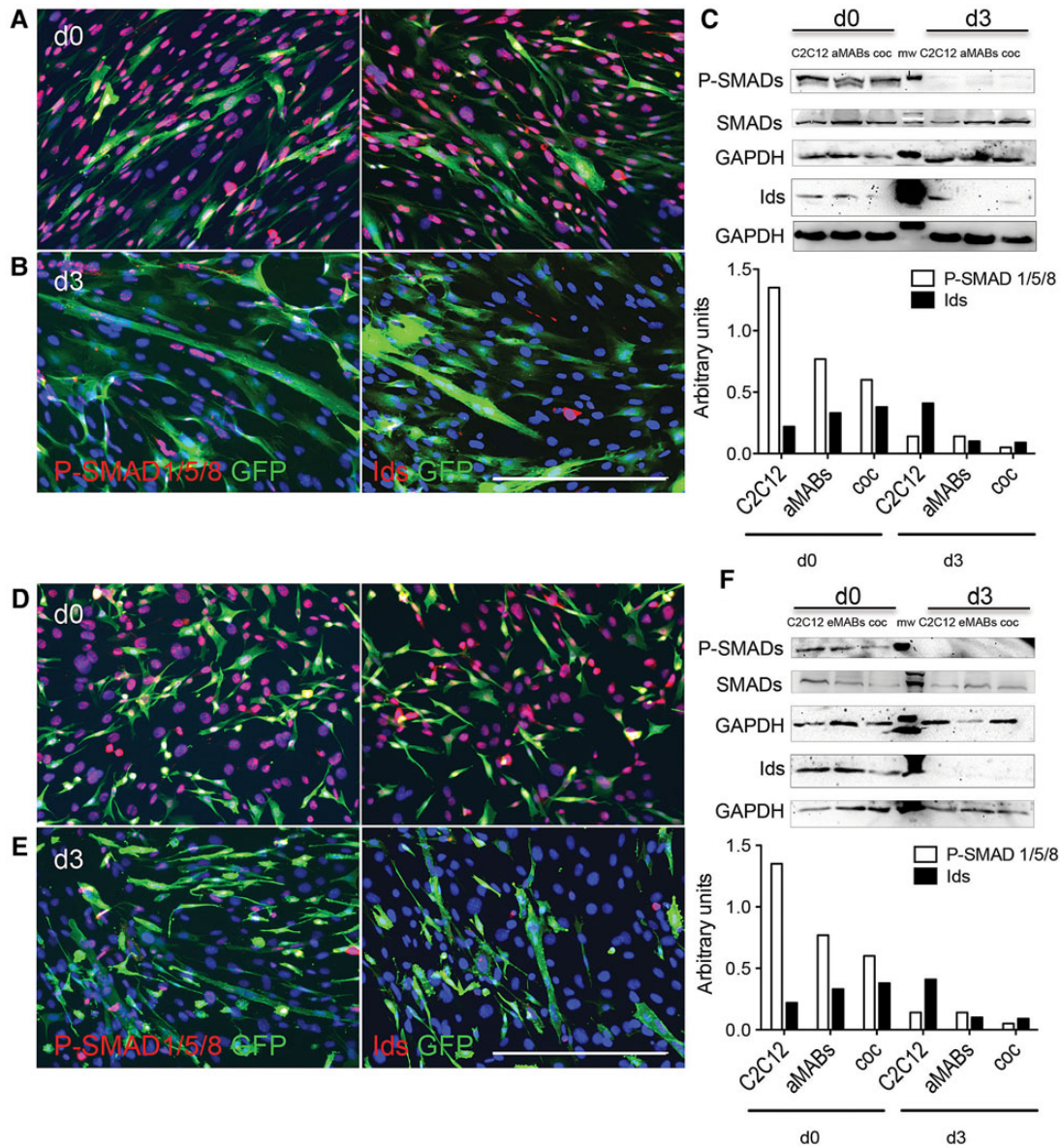
Figure 2 Nuclear P-SMAD1/5/8 and ID proteins in aMABs and eMABs. (**A**) IF analysis for P-SMAD1/5/8 (red) and GFP (green) (left panel) or ID proteins (red) and GFP (green) (right panel) in GFP+ aMABs and C2C12 co-cultures on Day 0. (**B**) IF analysis of co-cultures as in **A** on Day 3 of myogenic differentiation. (**C**) WB analysis (upper panel) and quantification (lower panel) of P-SMAD1/5/8 (P-SMADs), total SMAD1/5/8 (SMADs), and ID proteins normalized by GAPDH in C2C12, aMABs, and co-cultures on Day 0 and Day 3 of differentiation. (**D**) IF analysis for P-SMAD1/5/8 (red) and GFP (green) (left panel) or IDs (red) and GFP (green) (right panel) in GFP+ eMABs and C2C12 co-cultures on Day 0 of differentiation. (**E**) IF analysis of co-cultures as in **D** on Day 3 of myogenic differentiation. Nuclei were stained with Hoechst (blue). (**F**) WB (upper panel) and quantification (lower panel) of P-SMAD1/5/8 (P-SMADs), total SMAD1/5/8 (SMADs), and ID proteins normalized by GAPDH in C2C12, eMABs, and co-cultures on Day 0 and Day 3 of differentiation. Data are representative of three independent experiments. Scale bar, 500 μm.

embryos deficient for *Smad1/5* into SM22-positive cells (see Materials and methods and Supplementary Figure S6A). The growth rate of *Smad1/5*-null MABs was not significantly different from littermate control MABs (data not shown). However, a residual BMP–P-SMAD signal was detected by WB analysis in *Smad1/5*-null aMABs (Figure 4A and B) and eMABs (Figure 4D and E) although not detectable by IF analysis. A significant increase in the levels of SMAD8 protein (by WB, see Figure 4B and E) and mRNA (Figure 4C) was detected in the *Smad1/5*-null aMABs.

We then tested the differentiation ability of *Smad1/5*-null MABs in co-cultures with C2C12 cells (Figure 4F and G). The number of double-positive myotubes was not changed when using either *Smad1/5*-null aMABs or *Smad1/5*-null eMAB co-cultures compared with WT aMABs and eMABs (Figure 4H). Hence, the deletion of *Smad1/5*, often referred to as the major BMP-SMADs, is not sufficient to improve myotube differentiation of murine MABs. This prompted us to investigate in more detail the possible functions of SMAD8.
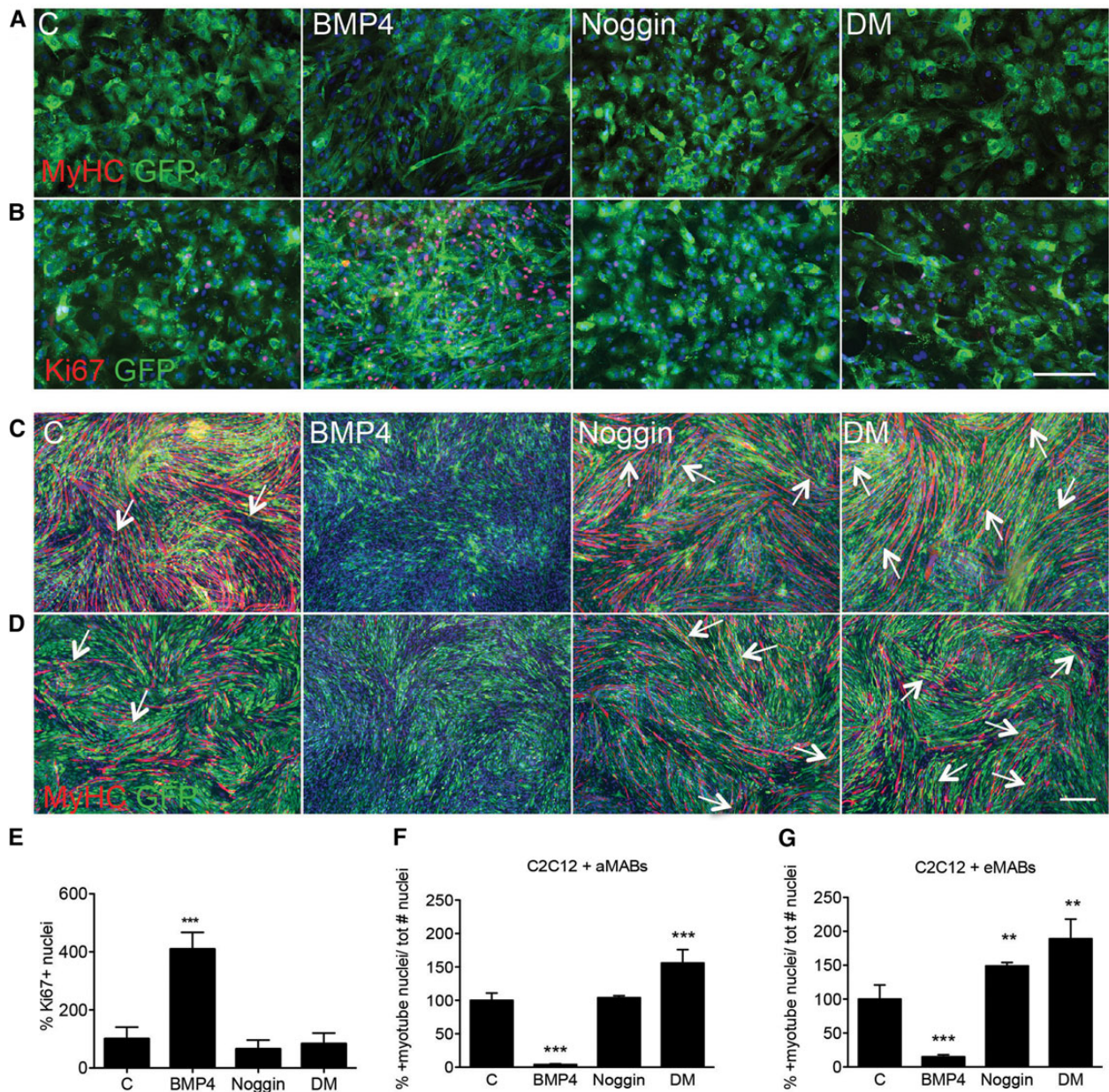
Figure 3 Interference with functional BMP signalling in aMABs and eMABs. (**A, B, E**) IF analysis for MyHC (red in **A**), Ki67 (red in **B**), and GFP (green) revealed that all treatments were not able to induce myogenic differentiation (up to 10 days) in GFP$^+$ aMABs (**A**). However, BMP administration resulted in increased number of Ki67-positive cells (**B** and **E**). (**C** and **D**) IF analysis for MyHC (red) and GFP (green) of GFP$^+$ aMABs (**C**) and eMABs (**D**) in co-cultures with C2C12 cells pre-treated with 200 ng/ml BMP4, 100 ng/ml Noggin, or 1 μM Dorsomorphin (DM), respectively, for 48 h, and consequently subjected to myogenic differentiation for 5 days. The arrows highlight GFP$^+$/MyHC$^+$ double-positive myotubes. Nuclei were stained with Hoechst (blue). (**F** and **G**) Fusion index of chimeric myotubes generated from aMABs (**F**) or eMABs (**G**) in co-culture experiments with different treatments is reported as percentage with respect to control conditions. **$P < 0.01$, ***$P < 0.001$ vs. C. Kruskal−Wallis test performed for both analyses scored $P = 0.0001$. Scale bar, 500 μm.

Smad8 knockdown in Smad1/5-null aMAB cells significantly improves their myogenic commitment

Smad8 knockdown was attested at both mRNA and protein levels in *Smad1/5*-null aMABs transfected with *Smad8*-esiRNA. *Smad8* mRNA progressively decreased to low levels (from 1 ± 0.23 to 0.2 ± 0.17 ΔΔCt; Figure 5A) 48 h after transfection, while the protein level

decreased by ∼90% (Figure 5B). The differentiation of *Smad1/5*-null MABs was induced in co-culture with C2C12 cells 48 h after transfection, corresponding to the peak of silencing of *Smad8*. IF analysis and MyHC levels detected by WB showed an improved differentiation for *Smad1/5*-null MABs silenced for *Smad8* (8esiRNA1/5-null aMABs), in comparison with *Smad1/5*-null and wild-type aMABs
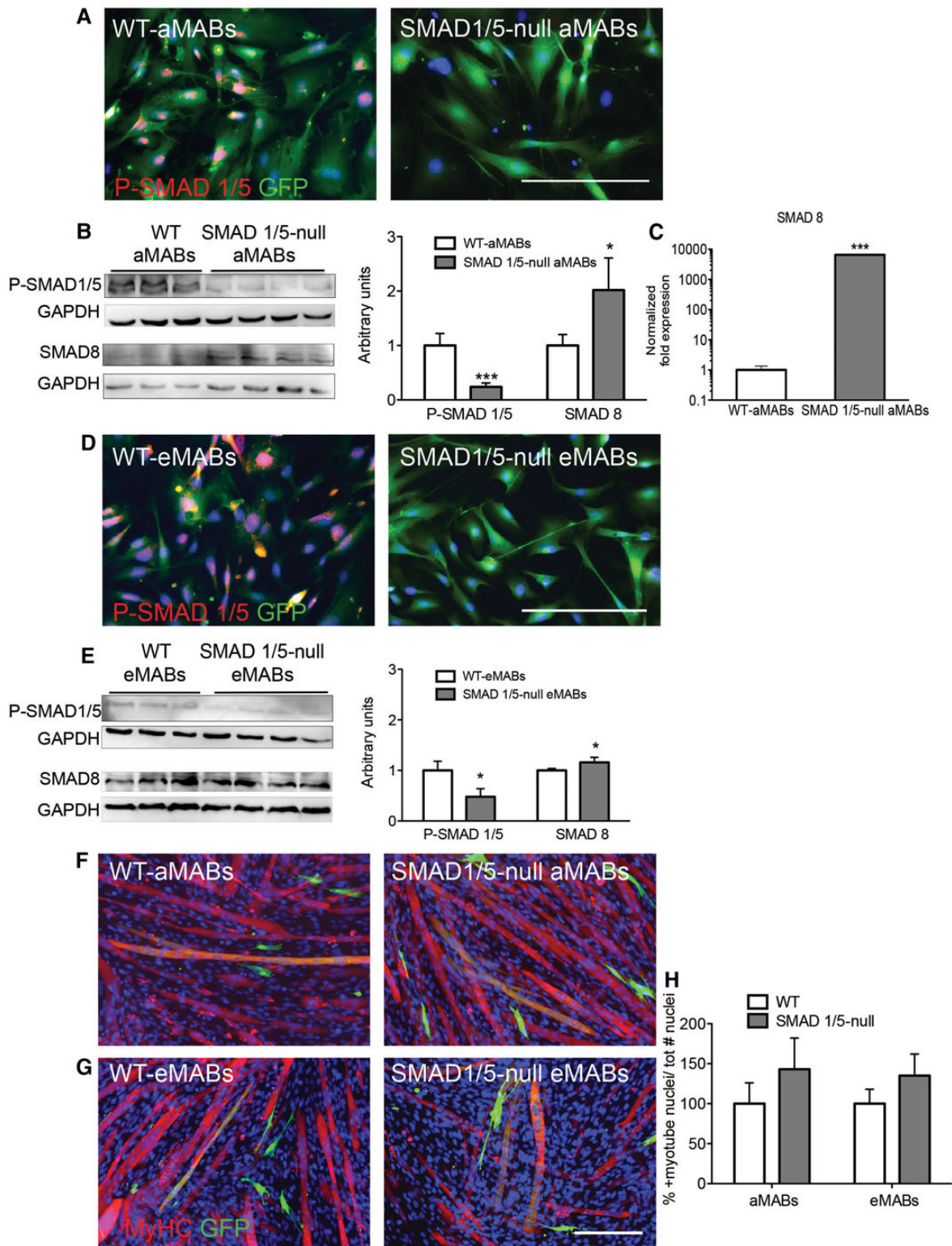
Figure 4 Characterization of murine *Smad1/5*-null aMABs and eMABs. (**A**) IF analysis for P-SMAD1/5/8 (red) and GFP (green) in *Smad1/5*-null and WT aMABs. (**B**) WB analysis (left panel) and quantification (right panel) of P-SMAD1/5/8 and SMAD8 levels normalized by GAPDH in *Smad1/5*-null aMABs. (**C**) RT-qPCR analysis of *Smad8* mRNA levels in *Smad1/5*-null aMABs. Data are expressed as fold induction compared with WT aMABs and normalized to steady-state mRNA levels of *Gapdh*, *Hprt*, and *Tbp* housekeeping genes. (**D**) IF analysis for P-SMAD1/5/8 (red) and GFP (green) in *Smad1/5*-null and WT eMABs. (**E**) WB analysis (left panel) and quantification (right panel) of P-SMAD1/5 and SMAD8 levels normalized by GAPDH in *Smad1/5*-null eMABs. (**F** and **G**) IF analysis for MyHC (red) and GFP (green) in *Smad1/5*-null aMABs (**F**) and eMABs (**G**) co-cultured with C2C12 (1:1) and subjected to myogenic differentiation for 5 days. (**H**) Fusion index of chimeric myotubes generated from *Smad1/5*-null aMABs (**F**) or eMABs (**G**) in co-culture experiments is reported as percentage with respect to WT MABs. *$P < 0.05$, ***$P < 0.001$ vs. WT. Scale bar, 500 μm.
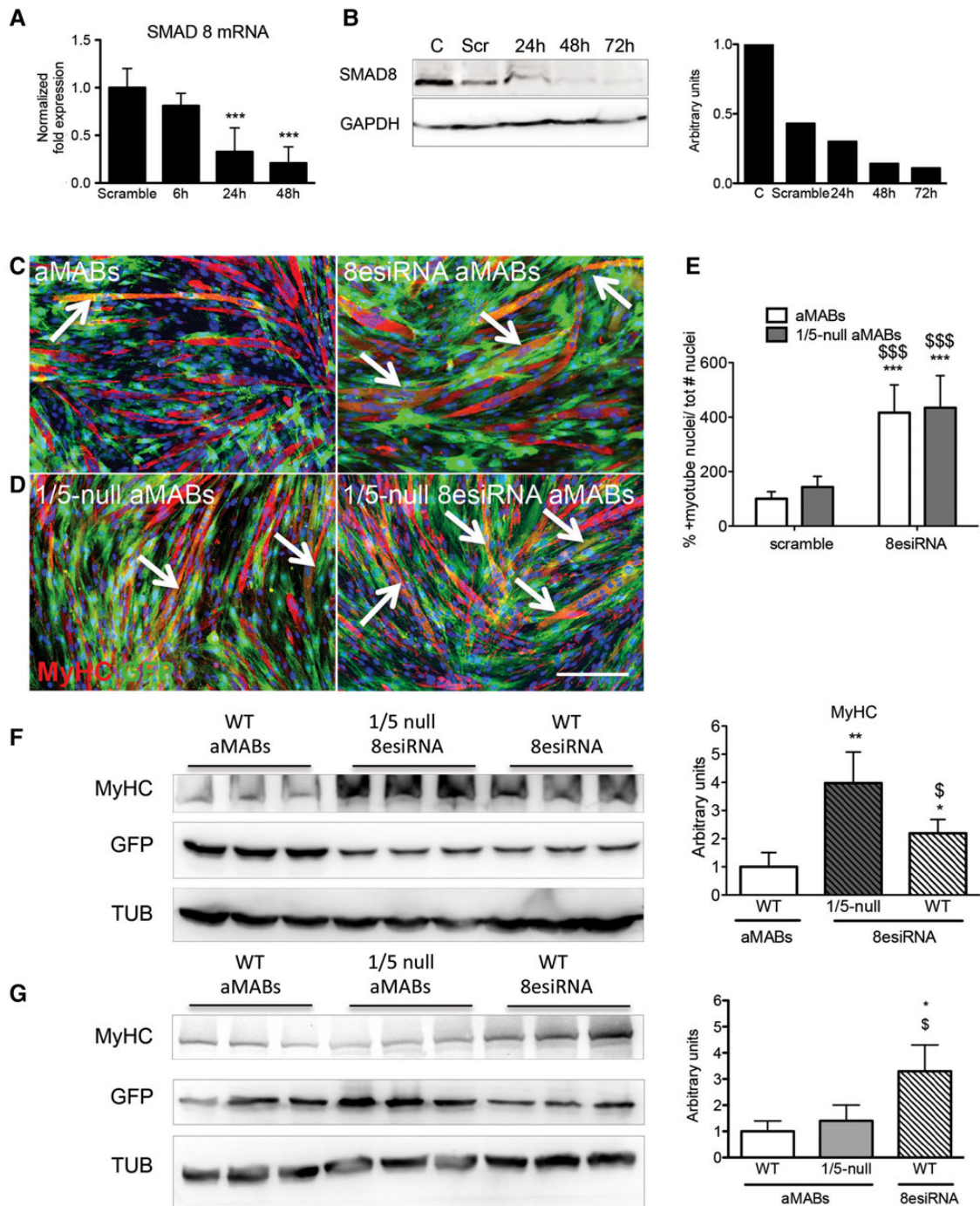
Figure 5 *Smad8* silencing by esiRNA in aMABs. (**A**) RT-qPCR analysis of *Smad8* transcript at 6, 24, and 48 h after *Smad8* silencing in *Smad1/5*-null aMABs. Data are expressed as fold expression compared with scramble treated cells and normalized to specific housekeeping genes (*Gapdh*, *Hprt*, and *Tbp*). Values are reported as mean $\pm$ SEM. (**B**) WB (left panel) and quantification (right panel) of SMAD8 protein levels normalized by GAPDH in *Smad1/5*-null aMABs silenced for *Smad8* for 24, 48, and 72 h. (**C**) IF analysis for MyHC (red) and GFP (green) in WT aMAB co-cultures (left panel) and WT aMAB silenced for *Smad8* co-cultures (indicated as 8esiRNA aMABs, right panel). (**D**) IF analysis for MyHC (red) and GFP (green) in *Smad1/5*-null aMAB co-cultures (indicated as 1/5-null aMABs, left panel) and *Smad1/5*-null aMABs silenced for *Smad8* co-cultures (1/5-null 8esiRNA aMABs, right panel). MyHC and GFP double-positive myotubes are highlighted with arrows. (**E**) Fusion index of chimeric myotubes generated from *Smad1/5*-null aMABs shown in **C** and **D** is reported as percentage with respect to scramble treated aMABs. (**F**) WB (left panel) and quantification (right panel) of MyHC and GFP levels normalized by TUB in WT aMABs, *Smad1/5*-null aMABs + *Smad8*esiRNA (indicated as 1/5-null 8esiRNA), and WT aMABs + *Smad8*esiRNA (indicated as WT 8esiRNA). (**G**) WB (left panel) and quantification (right panel) of MyHC and GFP levels normalized by TUB in WT aMABs, *Smad1/5*-null aMABs (indicated as 1/5-null aMABs), and *Smad8*esiRNA-treated WT aMABs (indicated as WT 8esiRNA). Data are representative of three independent experiments and values are expressed as mean $\pm$ SD; *$P < 0.05$, **$P < 0.01$, ***$P < 0.001$ vs. C; $^{\$}P < 0.05$, $^{\$\$}P < 0.01$, $^{\$\$\$}P < 0.001$ vs. respective controls. Scale bar, 500 μm.

(Figure 5C and D, Supplementary Figure S6B). Interestingly, the fusion index in chimeric myotubes from *Smad8*-esiRNA-treated aMABs (indicated as 8esiRNA aMABs) was comparable with 8esiRNA1/5-null aMABs (Figure 5E). This strongly suggests that *Smad*/8 signalling is not involved in fusion ability of *Smad1/5*-null MABs, although it positively affects myogenic protein production. Indeed, MyHC reaches higher levels in 8esiRNA1/5-null aMAB co-cultures compared with WT aMABs and 8esiRNA aMAB co-cultures (Figure 5F). The 90% reduction of *Smad8* reached in aMABs was sufficient to increase the MyHC protein level in co-culture experiments (Figure 5G). In addition, MAPKs were not substantially involved in this phenomenon (Supplementary Figure 6C and D). To our knowledge, this is the first report showing the importance of SMAD8 in the myogenic differentiation ability of aMAB cells. Finally, the results obtained strengthen the crucial role for the BMP−SMAD pathway in the maintenance of MAB stemness.

Homozygous aMABs carrying the Smad8.LacZ do not express Smad8 and display an enhanced myogenic commitment

Since SMAD8 is the critical factor for MAB differentiation, we isolated MABs from homozygous mice carrying the *Smad8.LacZ* reporter allele (Arnold et al., 2006). We confirmed the insertion of *LacZ* gene into *Smad8* by PCR analysis (Supplementary Figure S7A) and enzymatic assay (Supplementary Figure S7B) in the transgenic cells. We also proved that the *LacZ* cassette inserted into exon 2 of *Smad8* disrupted the endogenous coding sequence, resulting in the absence of SMAD8 protein (Supplementary Figure S7C). ID proteins were decreased in *Smad8.LacZ* MABs compared with controls, and proliferation ability was reduced (Supplementary Figure S7D). When cells were co-cultured with nLacZ C2C12 myoblasts in differentiation medium for 5 days, *Smad8.LacZ* MABs were able to form chimeric myotubes expressing MyHC, and the fusion index highly increased in comparison with controls (Supplementary Figure S7E−G). GFP$^+$ *Smad8.LacZ* aMABs (see Materials and methods) showed higher number of chimeric myotubes compared with WT GFP$^+$ aMABs in co-culture experiments (Supplementary Figure S7H) expressing β-gal and MyHC (Supplementary Figure S7I). In addition, C2C12-conditioned medium was able to induce myogenic commitment in *Smad8.LacZ* MABs, suggesting that they became C2C12 cell-contact independent for myogenic induction (Supplementary Figure S7J).

aMAB transplantation partially rescues αSG expression and muscle functionality in Sgca-null mice and contributes to muscle regeneration in acute damage

In order to assess the *in vivo* relevance of SMAD perturbation in skeletal muscle, DM-treated aMABs (aMABs+DM) were transplanted intramuscularly in 4 month-old *Sgca*-deficient (*Sgca*-null) mice (Duclos et al., 1998). Upon injection into the skeletal muscle of *Sgca*-null mice, GFP$^+$ aMABs engrafted into newly formed fibres (assessed by IF and histochemical analyses, Supplementary Figure S8A and B). aMAB+DM cells were able to give rise to a high number of GFP$^+$ fibres compared with untreated ones (Supplementary Figure S8C). Treatment with DM resulted in an increased αSG protein rescue in aMAB-injected muscles of *Sgca*-null mice (Figure 6A and B).

The treated mice were subjected to gait analysis (30 days after cell injection) and treadmill test (15 and 30 days after cell injection). After 30 days, aMAB-injected mice showed an increment in functional outcome when compared with sham-operated *Sgca*-null mice. Intriguingly, the effect was even more pronounced after aMABs+DM injection (Figure 7A). *Sgca*-null mice injected with aMABs were able to run for significantly longer period and distance than sham-operated *Sgca*-null mice (Figure 7B). Pre-treatment with DM further ameliorated the performances, as shown in Figure 7B and C.

We further performed aMAB transplantation experiments in crushed TA muscles of nude mice (Supplementary Figure S9). In this acute model of muscle regeneration, we evaluated the effect of BMP transient activation and inhibition on aMAB ability to directly contribute to regeneration post-injuries. After 20 days from the CTX injury, the number of GFP-positive fibres was significantly increased in TA treated with aMABs exposed to DM and Noggin (Supplementary Figure S9A, A′, and C). The second injury (on Day 20 from the first injury), to evaluate a further cycle of regeneration, resulted in the presence of GFP-positive fibres in all treated mice; however, no differences were observed among the different groups (Supplementary Figure S9B, B′, and C).

These results confirm that the inhibition of SMAD-mediated BMP signalling improves the therapeutic potential of aMABs.

BMP signalling also regulates stemness of the human MAB

We expanded the studies described above to hMABs currently involved in a clinical trial (EudraCT No. 2011-000176-33). Unlike murine MABs, hMABs spontaneously form myotubes in differentiating conditions (Dellavalle et al., 2007). MyHC$^+$ myotubes were formed 15 days after the differentiation induction (Figure 8A and B). Like murine MABs, the differentiation of hMABs was prevented as long as SMAD1/5/8 were phosphorylated and the ID proteins were present (Figure 8C). From the onset of differentiation, these P-SMAD1/5/8 and ID signals disappeared (Figure 8D−F). Treatment with Noggin or DM increased the myotube formation in differentiating hMABs (Figure 8G), confirming a comparable role of BMP signalling in murine and human MABs. As expected, treatment with BMP4 dropped the fusion index of hMABs dramatically with respect to control conditions (Figure 8H).

These results strongly point out a common and similar effect of BMP signalling in both murine and human MABs. Furthermore, these data suggest that perturbation of BMP signalling can improve the myogenic potential of hMABs.

Discussion

We provide new insights regarding the previously documented myogenic potential of MABs (Sampaolesi et al., 2003; Dellavalle et al., 2007), which are vessel-associated cell types now used in a phase-1 clinical trial (EudraCT #2011-000176-33) for the treatment of DMD patients. Here, we investigated the involvement of BMP and BMP−SMAD signalling in MAB myogenic commitment. This pathway is important in several cell processes, tissues, and organs, including cell behaviour in angiogenesis (Umans et al., 2007; Moya et al., 2012) and cell differentiation in myogenesis
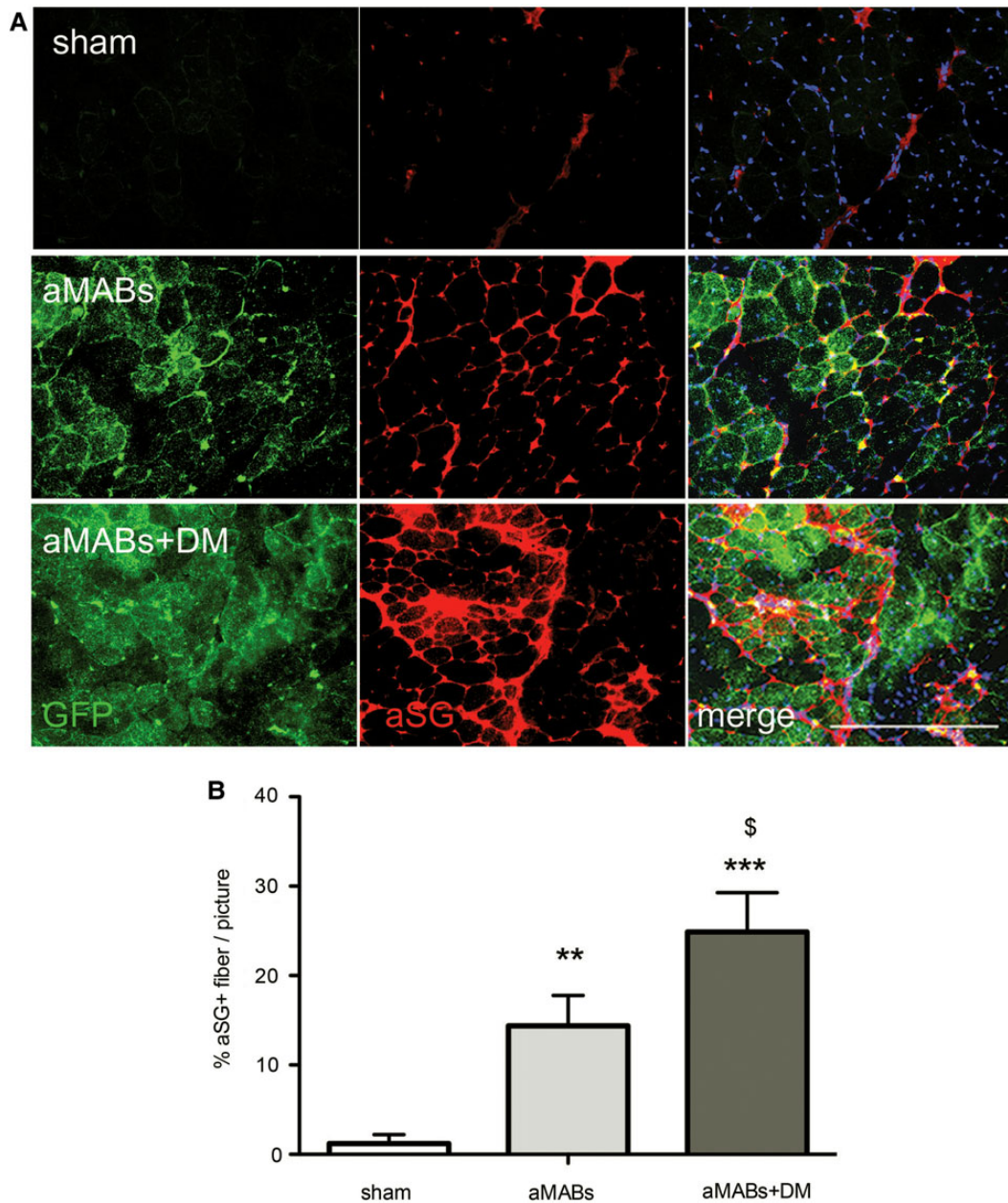
Figure 6 aMABs differentiation into αSG⁺ fibres. (**A**) IF analysis for αSG (red) and GFP (green) in *Sgca*-null muscles injected with GFP⁺ aMABs (aMABs, middle panels) or GFP⁺ aMABs pretreated with DM during 48 h (aMABs+DM, lower panels). Upper panels showed sham treated muscles. (**B**) Quantification of the αSG⁺ fibres in sham (*Sgca*-null) and cell-treated dystrophic muscles. **$P < 0.01$, ***$P < 0.001$ vs. *Sgca*-null mice; $^{\$}P < 0.05$ vs. aMABs-injected mice. Scale bar, 500 μm.

(Velasco et al., 2008). Previously, Tagliafico et al. (2004) reported that TGFβ/BMP signalling activates smooth muscle/bone differentiation programmes in embryonic MABs. We now stimulate receptor-mediated SMAD1/5/8 phosphorylation by administering BMP4 to embryonic and adult MABs under myogenic differentiation conditions. This results in the blocking of MAB differentiation, likely induced from P-SMAD1/5/8 and ID nuclear localization (Lin et al., 2000; Clever et al., 2010), thereby promoting cell proliferation as observed in SCs (Ono et al., 2011). When SMAD activation is prevented by Noggin or DM addition, MAB cells start to differentiate.

This suggests the intriguing possibility of using the modulation of BMP signalling, at multiple levels of the signal transduction cascade. Indeed, DM treatment boosts MAB myogenic potential and simultaneously improves their safety, by avoiding BMP-dependent stimulation of cell proliferation. Interestingly, under our conditions, SMAD1/5 are not the critical proteins responsible for MAB cell stemness, since *Smad1/5*-null murine MABs are able to grow equally as the wild-type counterparts. In addition, the differentiation ability of these *Smad1/5* deficient MABs is not further compromised. *Smad1/5*-null mice do not have skeletal muscle defects, and no
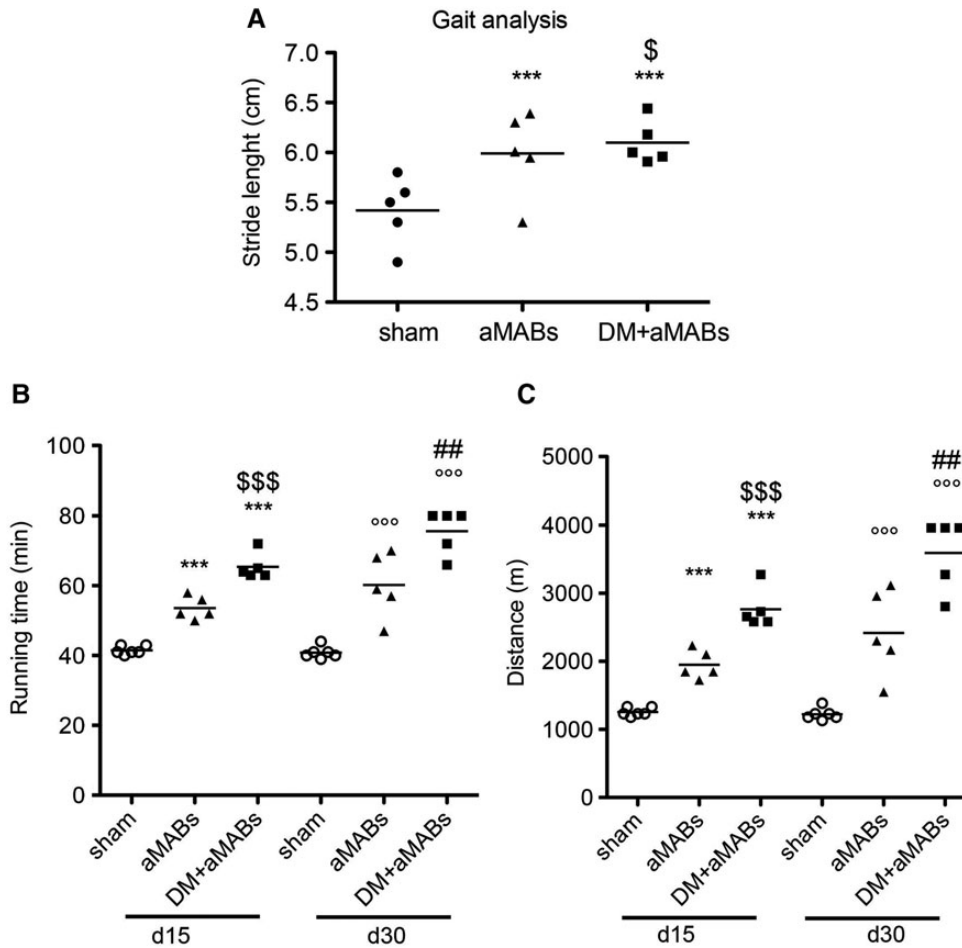
Figure 7 Functional analysis of aMAB-injected *Scga*-null mice. Gait (**A**) and treadmill (**B**) analyses of *Scga*-null mice injected with aMABs or aMABs pretreated with DM for 48 h (indicated as aMABs+DM). Treadmill tests were performed at two different time points (15 and 30 days after aMABs or aMABs+DM injections). ***$P < 0.001$ vs. *Sgca*-null Day 15; °°°$P < 0.01$ vs. *Sgca*-null Day 15; $^$P < 0.05$, $^{$$}P < 0.01$, $^{$$$}P < 0.001$ vs. aMABs. Kruskal–Wallis test performed for both analysis scored $P = 0.0012$.

differences in muscle weight and structure were observed. This is possibly due to a residual SMAD1/5 activity or most likely due to the compensation by SMAD8 whose mRNA and protein levels in *Smad1/5*-null pericytes were found increased. When *Smad8* is strongly downregulated (up to 90% reduction of the normal level) in WT aMABs, cells show increased differentiation ability, resulting in higher MyHC levels. This myogenesis induction is even further enhanced by *Smad8* knockdown in a *Smad1/5*-null setting. SMAD8 represents a novel candidate target for the improvement of MAB myogenic potential. Consistent with our data, abnormal pulmonary vessel remodelling and smooth muscle cell aberrations were reported in *Smad8*-null embryos (Huang et al., 2009). To date, no information has been available on pericyte myogenic ability from *Smad8*-null mice, although adult *Smad8* homozygous mutant mice are viable and fertile (Arnold et al., 2006). We now have filled this gap providing evidence that *Smad8.LacZ* MABs are able to undergo myogenic differentiation independently by C2C12 cell contact. This further supports our previous results obtained from *Smad8* knockdown experiments.

Pre-treating MAB cells with DM results in proliferation arrest and, when transplanted *in vivo,* a better engraftment in dystrophic skeletal muscles. The previous beneficial effect observed in treatments with DM of cardiotoxin-injured muscles (Ono et al., 2009, 2010) may be explained by our work reported here. To further support this hypothesis, we found that GFP$^+$ myofibres were more abundant in skeletal muscle injected with DM-treated GFP$^+$ aMABs, compared with those injected with untreated cells. The dose of DM we used was effective in decreasing the phosphorylation of SMAD1/5/8 (Yu et al., 2008), but appeared at the same time too low to inhibit certain kinases (Boergermann et al., 2010; White et al., 2013). Here, the functional read-out of the engraftment of MABs has been convincingly demonstrated and documented, yielding ameliorated performances by animals injected with DM-treated MABs compared with those injected with non-treated MABs. This was confirmed in both acute and chronic models of muscle regeneration.

Finally, the importance of SMAD1/5/8 signalling has also been demonstrated here in human MABs. These showed a similar ability
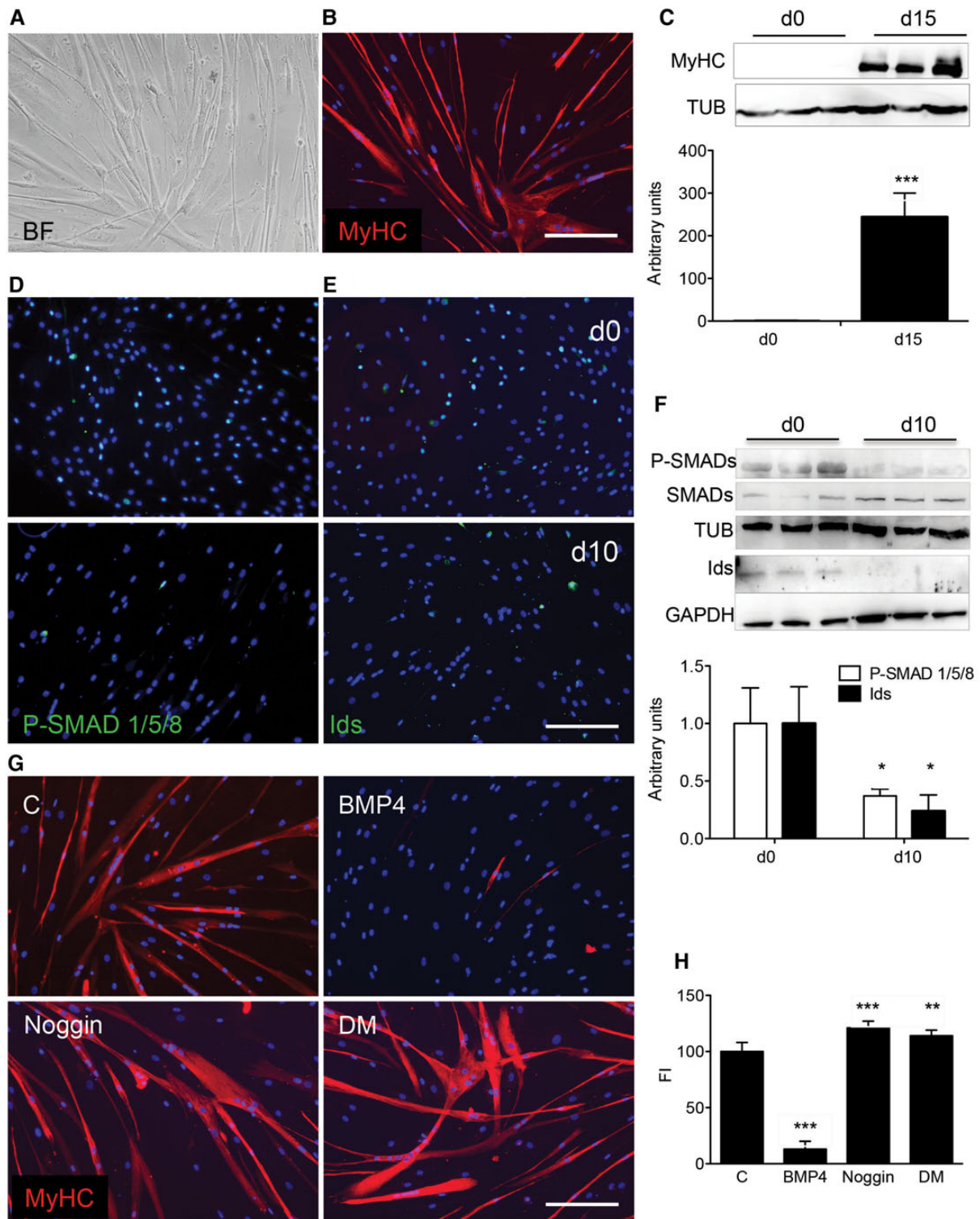
Figure 8 *In vitro* differentiation of human MABs. (**A** and **B**) hMABs cultivated for 15 days in differentiation medium generated myotubes (bright field, **A**) expressing MyHC (in red, right panel, **B**). (**C**) WB (upper panel) and quantification (lower panel) for MyHC normalized for tubulin (TUB) in hMAB cultures on Day 0 and 15 of differentiation. ***$P < 0.001$ vs. d0. (**D** and **E**) IF analysis in hMAB culture on Day 0 and 10 of differentiation for P-SMAD1/5/8 (green; upper and lower panels, **D**) or ID proteins (green; upper and lower panels, **E**). (**F**) WB (upper panel) and quantification (lower panel) of P-SMAD1/5/8 (indicated as P-SMADs) normalized for total SMAD1/5/8 (SMADs) and tubulin (TUB); ID proteins were normalized for GAPDH values. *$P < 0.05$ vs. d0. (**G**) IF analysis for MyHC (red) in hMABs cultures (C) treated for 72 h with 200 ng/ml of BMP4 (BMP4), with 100 ng/ml Noggin (Noggin) or 1 μM Dorsomorphin (DM), and consequently induced to differentiate for 15 days. Note that BMP4 completely abolished hMAB differentiation into myotubes. (**H**) Fusion index was calculated in all different treated cultures. Nuclei were stained with Hoechst. Data are representative of three independent experiments and values are expressed as mean ± SD, represented as percentage of C. **$P < 0.01$, ***$P < 0.001$ vs. C. Kruskal−Wallis test scored $P = 0.0001$. Scale bar, 500 μm.

to differentiate into myotubes when treated with DM. The interesting notion emerging from this work is the combination of human MABs and DM to improve myogenic commitment, but further studies are needed to evaluate the effect of DM pre-treatments *in vivo*. In addition, novel DM-like molecules (DMH1, DMH2, DMH3, and DMH4, and others) that are more specific and thereby less prone to induce side effects (like inhibition of other TGFβ family type I receptors, a number of protein kinases, or VEGF pathways) have been reported (Hao et al., 2010). It will be of great interest to test whether these compounds also improve myogenic differentiation.

Materials and methods

Cell isolation and culture

All animal procedures were performed according to the guidelines of the Animal Welfare Committee of KU Leuven and Belgian/European legislation. Adult, embryonic, and cardiac mesoangioblasts (aMABs, eMABs, and dMABs, respectively) were sorted for AP$^+$/live staining (Gibco-Life Technologies) as described previously (Crippa et al., 2011; Quattrocelli et al., 2011) and transfected with Sleeping Beauty transposon to induce GFP expression. Transfections were carried out using a non-liposomal lipid reagent suitable for primary cells (Effectene, Qiagen). After sorting, the GFP$^+$ cells were cultured on collagen-coated dishes (Sigma-Aldrich) and maintained in Dulbecco's modified Eagle's medium (DMEM)-high glucose, 20% fetal bovine serum, supplemented with 1 mg/ml of sodium pyruvate, 1 IU/ml of penicillin and streptomycin, 20 μM L-glutamine, and 1 mg/ml of non-essential amino acids. The plates were incubated at 37°C, 5% CO_2, 5% O_2, and the medium was refreshed every 2 days.

Smad1/5-null MABs were isolated from hindlimb skeletal muscle of 6-week-old mice (*Smad1/5*-null aMABs) and from the dorsal aorta of E10.5 mouse embryos (*Smad1/5*-null eMAB). Homozygous mice for floxed (fl) *Smad1* (Tremblay et al., 2001) and *Smad5* (Umans et al., 2003) alleles (*Smad1$^{fl/fl}$;Smad5$^{fl/fl}$*) and a RCE GFP Cre-reporter allele (Sousa et al., 2009) (*Smad1$^{fl/fl}$;Smad5$^{fl/fl}$;RCE$^{fl/fl}$*) were mated with a *SM22-Cre-* mouse (Holtwick et al., 2002) (actively present in smooth muscle cells and pericytes; see Supplementary Figure S6A) heterozygous for floxed *Smad1* and *Smad5* (*SM22-Cre$^{+/O}$;Smad1$^{fl/+}$;Smad5$^{fl/+}$*) to obtain complete deletion of the four floxed alleles of *Smad1* and *Smad5* in smooth muscle cells and pericytes (*SM22-Cre$^{+/O}$;Smad1$^{-/-}$;Smad5$^{-/-}$;RCE$^{fl/O}$*) in 12.5% of the resulting offspring. Genotyping of *Smad1* and *Smad5* floxed vs. recombined alleles was performed as described (Tremblay et al., 2001; Umans et al., 2007; Monteiro et al., 2008). All mice used in these experiments have a variable mixed background (CD1, 129/Ola, and C57BL6).

Human MABs (hMABs) were generated by F.v.T. and I.F.M.d.C. hMABs were isolated from biopsy culture according to reported conditions (Quattrocelli et al., 2012) and were maintained in Iscove's Modified Dulbecco's Media (IMDM), 10% FBS, supplemented with 1 mg/ml of sodium pyruvate, 1 IU/ml of penicillin and streptomycin, 20 μM L-glutamine, 1 mg/ml of non-essential amino acids, 5 ng/ml of recombinant human fibroblast growth factor-basic (FGF-2, PeproTech, London, UK), and 1× Insulin-Transferrin-Selenium.

For differentiation experiments, murine MABs were plated alone, or as specified in 1:1 ratio with C2C12 myoblasts; in case of hMABs, cells were always plated alone. Depending on the experiments, cells were pre-treated (48 h) or not with 200 ng/ml of BMP4, 100 ng/ml of Noggin (R&D Systems Europe Ltd.), or 1 μM Dorsomorphin (DM; Sigma-Aldrich), respectively, or with vehicle as control. When confluence was reached, the differentiation was induced by shifting medium to DMEM-high glucose supplemented with 2% horse serum, 1 mg/ml of sodium pyruvate, and 1 IU/ml of penicillin and streptomycin (referred to as differentiation medium). Myogenic induction was evaluated on Day 3, 5, and in specific tests on Day 10 (murine MAB spontaneous differentiation, Figure 3A) or on Day 14 (hMAB myogenic differentiation, Figure 8A and B).

Smad8 knockdown

In order to efficiently knockdown murine *Smad8*, endoribonuclease-prepared siRNAs against *Smad8* (in fact named *Smad9* esiRNAs; Sigma-Aldrich) were applied following the manufacturer's instructions. Briefly, aMABs and *Smad1/5*-null aMABs were transfected with mouse *Smad9* esiRNA using Lipofectamine-2000 and Opti-MEM. At different time points after transfection, cells were lysed for RNA extraction or western blot (WB) analysis. RNA Mini Kit was used for RNA isolation, and genomic DNA traces were removed with Turbo DNase, following manufacturer's instructions. One microgram of RNA was reverse-transcribed with the SuperScript III kit. The resulting cDNA (1:4 dilution) was transferred in a 384-well plate pre-filled with 250 nM primers (*Smad8*-Fw: CAGCATCTTTGTCCAGAGCC, *Smad8*-Rev: AAAGCTCATCCGAATCGT GC; *glyceraldehyde-3-phosphate dehydrogenase*, *Gapdh*-Fw: TGGT GAAGGTCGGTGTGAAC, *Gapdh*-Rev: GCTCCTGGAAGATGGTGATGG; *TATA-box binding protein*, *TBP*-Fw: CAAACCCAGAATTGTTCTCCTT, *TBP*-Rev: ATGTGGTCTTCCTGAATCCCT; *hypoxanthine guanine phosphoribosyl transferase*, *HPRT*-Fw: TGGATACAGGCCAGACTTTGTT, *HPRT*-Rev: CAGATTCAACTTGCGCTCATC) and Platinum Sybr Green Mix to a final volume of 10 μl/well. The RT-qPCR was performed for 40 cycles (95°C, 15 sec; 58°C, 45 sec) and read on a ViiA 7 qPCR plate reader.

In vivo experiments

Intramuscular injections of 2×10^5 GFP$^+$ aMAB or aMAB cells pre-treated for 48 h with 5 μM Dorsomorphin (DM-aMABs) were performed in *Sgca*-null (C57/BL6 background) dystrophic mice (4-month-old, $n = 8$ for each group), which were generated by the group of K.P. Campbell (University of Iowa, IA, USA) (Duclos et al., 1998). During the entire treatment, mice were maintained with cyclosporine (Sandimmune Cyclosporine, Novartis; 10 mg/kg). Functional assays were performed on the same mice 15 and 30 days post-injection and compared to sham-operated mice (saline solution injected mice) (Hampton et al., 2011; Consalvi et al., 2013). The mice were introduced to the treadmill belt and testing conditions before the actual recordings (motor speed set to zero, for 5 min). Later on, the motor speed was set to 10 m/min, with a 1 m/min increase and an uphill inclination of 10°, till exhaustion and >10s stop. For the gait analysis test, as previously described (Hamers et al., 2006), the animals were placed in a corridor (1 m long and

8.5 cm wide) and allowed to move freely across the walkway. Tracks with a straight walking direction and without any interruption or hesitation were acquired (5 runs from each animal). Values from the analysed tracks for each mouse were averaged and used for data processing. After sacrificing the mice, *tibialis anterior* (TA), *gastrocnemius* (GSN), and *quadriceps* (QD) muscles were excised and stored at $-80°$C for further analysis.

Intramuscular injections of 2×10^5 GFP$^+$ aMAB or aMAB cells pretreated for 48 h with 200 ng/ml of BMP4, 100 ng/ml of Noggin, or 5 μM Dorsomorphin (as previously described) were performed in 6-week-old male athymic nude mice (NMRI, nu/nu, Charles River; $n = 6$ for each group). Mice received a 10 μM solution of cardiotoxin (CTX, *Naja Mossambica Mossambica*, Sigma-Aldrich) in the TA of each hind limb at 48 h before the cell injection and again after 20 days. After the *in vivo* experiments, the mice were sacrificed by cervical dislocation and TA muscles were processed for histological analysis.

Immunofluorescence analysis

Tissues (7 μm) and cells were fixed with 4% paraformaldehyde (PFA, Polysciences Europe GmbH) in PBS and permeabilized with 0.2% Triton X-100 in PBS containing 1% (*w/v*) bovine serum albumin (BSA). A blocking solution containing donkey serum (1:10 dilution in PBS; VWR) was applied, and primary antibodies (reported hereafter) were incubated overnight in PBS supplemented with 1% BSA. Secondary Alexa Fluor donkey antibodies were diluted at 4 μg/ml in PBS supplemented with 1% BSA, and the nuclei were counterstained with 10 μg/ml Hoechst. Fluor Save reagent (Millipore, Chemicon) was used as mounting medium. Images were acquired using an Eclipse Ti inverted microscope (Nikon). The fusion index (e.g. the number of myotube nuclei vs. the total number of nuclei) for hMAB cultures or the percentage of nuclei in GFP$^+$ myotubes vs. the total number of nuclei for all co-cultures was calculated for a minimum of four random fields in each condition ($n = 3$).

The primary antibodies and their dilutions were as follows: 1:300 rabbit anti-GFP (Life Technologies) or 1:500 goat anti-GFP (Abcam; depending on the specific use for IF or WB analyses and on the combination with other antibodies), 1:3 mouse anti-MyHC (Developmental Studies Hybridoma Bank, DSHB, clone MF20), 1:1000 rabbit anti-P-SMAD1/5/8 or rabbit anti-P-SMAD1/5 (Cell Signalling), 1:200 rabbit anti-ID1 (Santa Cruz Biotechnology).

Immunohistochemistry

Sections (7 μm) were pre-incubated in peroxidase blocking solution, followed by an overnight incubation at 4°C with 1:500 goat anti-GFP (Abcam). The sections were then washed and incubated with 1:750 biotinylated anti-goat antibody (VECTOR), and finally with 1:100 Streptavidin-HRP (VECTOR). The antibody staining was visualized with 0.05% DAB (Sigma-Aldrich) and sections were mounted with Fluor Save reagent (Millipore, Chemicon).

Lacz staining

Smad8.LacZ aMABs and *nLacZ* C2C12 cells were fixed for 15–30 min in PFA and washed three times for 15 min with NP40 and deoxycholate. The LacZ staining was performed at 37°C using the X-gal solution (Sigma-Aldrich), and the intensity of the signal was monitored under inverted microscope (1–2 h).

Western blotting

Western blotting (WB) analysis was performed on lysates from tissue or cells in RIPA buffer (Sigma-Aldrich) supplemented with 10 mM Sodium Fluoride, 0.5 mM Sodium Orthovanadate, 1:100 Protease Inhibitor Cocktail, and 1 mM Phenylmethylsulfonyl Fluoride (PMSF). Equal amounts of protein (40 μg) were heat-denatured in sample-loading buffer (50 mM Tris−HCl, pH 6.8, 100 mM DTT, 2% SDS, 0.1% bromophenol blue, 10% glycerol), resolved by SDS-polyacrylamide gel electrophoresis, and then transferred to nitrocellulose membranes (Protran, Nitrocellulose membrane, Sigma-Aldrich). The filters were blocked with Tris-buffered saline (TBS) containing 0.05% Tween and 5% non-fat dry milk (Sigma-Aldrich) and then incubated overnight with the indicated dilutions of different primary antibodies: 1:10 mouse anti-MF20 (Developmental Studies Hybridoma Bank, DSHB), 1:1000 rabbit anti-P-SMAD1/5/8 (hereafter indicated as anti-P-SMADs) or 1:1000 rabbit anti-P-SMAD1/5 (Cell Signalling), 1:500 rabbit SMAD1/5/8 (hereafter indicated as anti-SMADs; Thermo Fisher Scientific Inc.), 1:100 rabbit anti-ID1 (Santa Cruz Biotechnology), 1:100 goat anti-SMAD8 (Sigma Aldrich). All secondary horseradish peroxidase (HRP)-conjugated antibodies (Santa Cruz Biotechnology) were diluted 1:5000 in TBS-Tween and 2.5% non-fat dry milk (Sigma-Aldrich). After incubation with SuperSignal Dura Chemiluminescence substrate (Thermo Scientific), the polypeptide bands were detected with GelDoc chemiluminescence detection system (BioRad). Quantitation was performed on gels loaded and blotted in parallel, and relative densitometry was obtained by normalizing the protein band vs. background and housekeeping protein (Glyceraldehyde 3-phosphate dehydrogenase, GAPDH, Sigma-Aldrich; Tubulin beta, TUB clone KMX-1, Millipore, Merck KGaA) using the QuantityOne software (BioRad).

RT-qPCR

Conventional RT-qPCR analysis for the mRNA levels of *SM22* in different cell types has been performed using primers and following conditions described previously (Sohni et al., 2012). *LacZ* gene expression from *Smad8.LacZ* mice was established with the following primers: *LacZ*-Fw: TTGAAAATGGTCTGCTGCTG, *LacZ*-Rev: TATTGGC TTCATCCACCACA. PCR products (expected as an amplified fragment of 226 bp) were separated on 2% agarose gels and visualized with SybrSafe (Life Technologies) on a GelDoc UV detection system (BioRad).

Statistical analysis

All results were expressed as mean $\pm$ SD, with the exception of gene expression (mean $\pm$ SEM). Representative WBs were selected from independent experiments. When data distribution approximated normality and two groups were compared, a Student's *t*-test was used. When three or more groups were compared, a two-way ANOVA was used. In case of non-normal distribution of the data pools, such as for statistical comparison of the differences between percentage values, a Kruskal−Wallis one-way analysis of

variance by rank test was used. All statistical tests were performed via Prism software (GraphPad).

Conflict of interest: none declared.

References

Acharyya, S., Villalta, S.A., Bakkar, N., et al. (2007). Interplay of IKK/NF-κB signaling in macrophages and myofibers promotes muscle degeneration in Duchenne muscular dystrophy. J. Clin. Invest. *117*, 889–901.

Arnold, S.J., Maretto, S., Islam, A., et al. (2006). Dose-dependent Smad1, Smad5 and Smad8 signaling in the early mouse embryo. Dev. Biol. *296*, 104–118.

Beets, K., Huylebroeck, D., Moya, I.M., et al. (2013). Robustness in angiogenesis: notch and BMP shaping waves. Trends Genet. *29*, 140–149.

Bernasconi, P., Torchiana, E., Confalonieri, P., et al. (1995). Expression of transforming growth factor-β 1 in dystrophic patient muscles correlates with fibrosis. Pathogenetic role of a fibrogenic cytokine. J. Clin. Invest. *96*, 1137–1144.

Boergermann, J.H., Kopf, J., Yu, P.B., et al. (2010). Dorsomorphin and LDN-193189 inhibit BMP-mediated Smad, p38 and Akt signalling in C2C12 cells. Int. J. Biochem. Cell Biol. *42*, 1802–1807.

Chang, J., Most, D., Bresnick, S., et al. (1999). Proliferative hemangiomas: analysis of cytokine gene expression and angiogenesis. Plast. Reconstr. Surg. *103*, 1–9; discussion 10.

Chen, Y.W., Nagaraju, K., Bakay, M., et al. (2005). Early onset of inflammation and later involvement of TGFβ in Duchenne muscular dystrophy. Neurology *65*, 826–834.

Christov, C., Chretien, F., Abou-Khalil, R., et al. (2007). Muscle satellite cells and endothelial cells: close neighbors and privileged partners. Mol. Biol. Cell *18*, 1397–1409.

Chun, J.L., O'Brien, R., Song, M.H., et al. (2013). Injection of vessel-derived stem cells prevents dilated cardiomyopathy and promotes angiogenesis and endogenous cardiac stem cell proliferation in mdx/utrn$^{-/-}$ but not aged mdx mouse models for duchenne muscular dystrophy. Stem Cells Transl. Med. *2*, 68–80.

Clever, J.L., Sakai, Y., Wang, R.A., et al. (2010). Inefficient skeletal muscle repair in inhibitor of differentiation knockout mice suggests a crucial role for BMP signaling during adult muscle regeneration. Am. J. Physiol. Cell Physiol. *298*, C1087–C1099.

Cohn, R.D., van Erp, C., Habashi, J.P., et al. (2007). Angiotensin II type 1 receptor blockade attenuates TGF-β-induced failure of muscle regeneration in multiple myopathic states. Nat. Med. *13*, 204–210.

Consalvi, S., Mozzetta, C., Bettica, P., et al. (2013). Preclinical studies in the mdx mouse model of duchenne muscular dystrophy with the histone deacetylase inhibitor givinostat. Mol. Med. *19*, 79–87.

Crippa, S., Cassano, M., Messina, G., et al. (2011). miR669a and miR669q prevent skeletal muscle differentiation in postnatal cardiac progenitors. J. Cell Biol. *193*, 1197–1212.

Dahlqvist, C., Blokzijl, A., Chapman, G., et al. (2003). Functional Notch signaling is required for BMP4-induced inhibition of myogenic differentiation. Development *130*, 6089–6099.

Dellavalle, A., Sampaolesi, M., Tonlorenzi, R., et al. (2007). Pericytes of human skeletal muscle are myogenic precursors distinct from satellite cells. Nat. Cell Biol. *9*, 255–267.

Duclos, F., Straub, V., Moore, S.A., et al. (1998). Progressive muscular dystrophy in α-sarcoglycan-deficient mice. J. Cell Biol. *142*, 1461–1471.

Feng, X.H., and Derynck, R. (2005). Specificity and versatility in tgf-β signaling through Smads. Annu. Rev. Cell Dev. Biol. *21*, 659–693.

Goumans, M.J., and Mummery, C. (2000). Functional analysis of the TGFβ receptor/Smad pathway through gene ablation in mice. Int. J. Dev. Biol. *44*, 253–265.

Hamers, F.P., Koopmans, G.C., and Joosten, E.A. (2006). CatWalk-assisted gait analysis in the assessment of spinal cord injury. J. Neurotrauma *23*, 537–548.

Hampton, T.G., Kale, A., Amende, I., et al. (2011). Gait disturbances in dystrophic hamsters. J. Biomed. Biotechnol. *2011*, 235354.

Hao, J., Daleo, M.A., Murphy, C.K., et al. (2008). Dorsomorphin, a selective small molecule inhibitor of BMP signaling, promotes cardiomyogenesis in embryonic stem cells. PLoS One *3*, e2904.

Hao, J., Ho, J.N., Lewis, J.A., et al. (2010). In vivo structure-activity relationship study of dorsomorphin analogues identifies selective VEGF and BMP inhibitors. ACS Chem. Biol. *5*, 245–253.

Holtwick, R., Gotthardt, M., Skryabin, B., et al. (2002). Smooth muscle-selective deletion of guanylyl cyclase-A prevents the acute but not chronic effects of ANP on blood pressure. Proc. Natl Acad. Sci. USA *99*, 7142–7147.

Huang, Z., Wang, D., Ihida-Stansbury, K., et al. (2009). Defective pulmonary vascular remodeling in Smad8 mutant mice. Hum. Mol. Genet. *18*, 2791–2801.

Jen, Y., Weintraub, H., and Benezra, R. (1992). Overexpression of Id protein inhibits the muscle differentiation program: in vivo association of Id with E2A proteins. Genes Dev. *6*, 1466–1479.

Katagiri, T., Akiyama, S., Namiki, M., et al. (1997). Bone morphogenetic protein-2 inhibits terminal differentiation of myogenic cells by suppressing the transcriptional activity of MyoD and myogenin. Exp. Cell Res. *230*, 342–351.

Katagiri, T., Imada, M., Yanai, T., et al. (2002). Identification of a BMP-responsive element in Id1, the gene for inhibition of myogenesis. Genes Cells *7*, 949–960.

Lin, C.Q., Singh, J., Murata, K., et al. (2000). A role for Id-1 in the aggressive phenotype and steroid hormone response of human breast cancer cells. Cancer Res. *60*, 1332–1340.

Linker, C., Lesbros, C., Stark, M.R., et al. (2003). Intrinsic signals regulate the initial steps of myogenesis in vertebrates. Development *130*, 4797–4807.

Monteiro, R.M., de Sousa Lopes, S.M., Bialecka, M., et al. (2008). Real time monitoring of BMP Smads transcriptional activity during mouse development. Genesis *46*, 335–346.

Moya, I.M., Umans, L., Maas, E., et al. (2012). Stalk cell phenotype depends on integration of Notch and Smad1/5 signaling cascades. Dev. Cell *22*, 501–514.

Oh, S.P., Seki, T., Goss, K.A., et al. (2000). Activin receptor-like kinase 1 modulates transforming growth factor-β 1 signaling in the regulation of angiogenesis. Proc. Natl Acad. Sci. USA 97, 2626–2631.

Ono, Y., Gnocchi, V.F., Zammit, P.S., et al. (2009). Presenilin-1 acts via Id1 to regulate the function of muscle satellite cells in a γ-secretase-independent manner. J. Cell Sci. 122, 4427–4438.

Ono, Y., Boldrin, L., Knopp, P., et al. (2010). Muscle satellite cells are a functionally heterogeneous population in both somite-derived and branchiomeric muscles. Dev. Biol. 337, 29–41.

Ono, Y., Calhabeu, F., Morgan, J.E., et al. (2011). BMP signalling permits population expansion by preventing premature myogenic differentiation in muscle satellite cells. Cell Death Differ. 18, 222–234.

Pangas, S.A., Li, X., Umans, L., et al. (2008). Conditional deletion of Smad1 and Smad5 in somatic cells of male and female gonads leads to metastatic tumor development in mice. Mol. Cell. Biol. 28, 248–257.

Quattrocelli, M., Palazzolo, G., Floris, G., et al. (2011). Intrinsic cell memory reinforces myogenic commitment of pericyte-derived iPSCs. J. Pathol. 223, 593–603.

Quattrocelli, M., Palazzolo, G., Perini, I., et al. (2012). Mouse and human mesoangioblasts: isolation and characterization from adult skeletal muscles. Methods Mol. Biol. 798, 65–76.

Quattrocelli, M., Costamagna, D., Giacomazzi, G., et al. (2014). Notch signaling regulates myogenic regenerative capacity of murine and human mesoangioblasts. Cell Death Dis. 5, e1448.

Reshef, R., Maroto, M., and Lassar, A.B. (1998). Regulation of dorsal somitic cell fates: BMPs and Noggin control the timing and pattern of myogenic regulator expression. Genes Dev. 12, 290–303.

Sampaolesi, M., Torrente, Y., Innocenzi, A., et al. (2003). Cell therapy of α-sarcoglycan null dystrophic mice through intra-arterial delivery of mesoangioblasts. Science 301, 487–492.

Sampaolesi, M., Blot, S., D'Antona, G., et al. (2006). Mesoangioblast stem cells ameliorate muscle function in dystrophic dogs. Nature 444, 574–579.

Sartori, R., Schirwis, E., Blaauw, B., et al. (2013). BMP signaling controls muscle mass. Nat. Genet. 45, 1309–1318.

Sohni, A., Mulas, F., Ferrazzi, F., et al. (2012). TGFβ1-induced Baf60c regulates both smooth muscle cell commitment and quiescence. PLoS One 7, e47629.

Sousa, V.H., Miyoshi, G., Hjerling-Leffler, J., et al. (2009). Characterization of Nkx6-2-derived neocortical interneuron lineages. Cereb. Cortex 19(Suppl 1), i1–i10.

Tagliafico, E., Brunelli, S., Bergamaschi, A., et al. (2004). TGFβ/BMP activate the smooth muscle/bone differentiation programs in mesoangioblasts. J. Cell Sci. 117, 4377–4388.

Tedesco, F.S., and Cossu, G. (2012). Stem cell therapies for muscle disorders. Curr. Opin. Neurol. 25, 597–603.

Tonlorenzi, R., Dellavalle, A., Schnapp, E., et al. (2007). Isolation and characterization of mesoangioblasts from mouse, dog, and human tissues. Curr. Protoc. Stem Cell Biol. Chapter 2, Unit 2B 1.

Tremblay, K.D., Dunn, N.R., and Robertson, E.J. (2001). Mouse embryos lacking Smad1 signals display defects in extra-embryonic tissues and germ cell formation. Development 128, 3609–3621.

Tzahor, E., Kempf, H., Mootoosamy, R.C., et al. (2003). Antagonists of Wnt and BMP signaling promote the formation of vertebrate head muscle. Genes Dev. 17, 3087–3099.

Ugarte, G., Cappellari, O., Perani, L., et al. (2012). Noggin recruits mesoderm progenitors from the dorsal aorta to a skeletal myogenic fate. Dev. Biol. 365, 91–100.

Umans, L., Vermeire, L., Francis, A., et al. (2003). Generation of a floxed allele of Smad5 for cre-mediated conditional knockout in the mouse. Genesis 37, 5–11.

Umans, L., Cox, L., Tjwa, M., et al. (2007). Inactivation of Smad5 in endothelial cells and smooth muscle cells demonstrates that Smad5 is required for cardiac homeostasis. Am. J. Pathol. 170, 1460–1472.

Velasco, S., Alvarez-Munoz, P., Pericacho, M., et al. (2008). L- and S-endoglin differentially modulate TGFβ1 signaling mediated by ALK1 and ALK5 in L6E9 myoblasts. J. Cell Sci. 121, 913–919.

White, J.P., Puppa, M.J., Gao, S., et al. (2013). Muscle mTORC1 suppression by IL-6 during cancer cachexia: a role for AMPK. Am. J. Physiol. Endocrinol. Metab. 304, E1042–E1052.

Yang, X., Castilla, L.H., Xu, X., et al. (1999). Angiogenesis defects and mesenchymal apoptosis in mice lacking SMAD5. Development 126, 1571–1580.

Yu, P.B., Hong, C.C., Sachidanandan, C., et al. (2008). Dorsomorphin inhibits BMP signals required for embryogenesis and iron metabolism. Nat. Chem. Biol. 4, 33–41.